Pharm Res (2012) 29:756–769
DOI 10.1007/s11095-011-0600-9

RESEARCH PAPER

Fabrication of Cisplatin-Loaded Poly(lactide-*co*-glycolide) Composite Microspheres for Osteosarcoma Treatment

Yan Li • Sierin Lim • Chui Ping Ooi

Received: 20 June 2011 / Accepted: 20 September 2011 / Published online: 7 October 2011

ABSTRACT

Purpose To reduce the toxicity and achieve a sustainable and controllable release of cisplatin (CDDP).

Methods CDDP was loaded onto Fe5 (Fe^{3+} doped hydroxyapatite at atomic ratio of $Fe_{added}/Ca_{added} = 5\%$) nanoparticles through surface adsorption. Subsequently, CDDP-loaded Fe5 nanoparticles (CDDP-Fe5) and/or CDDP were encapsulated into poly(lactide-*co*-glycolide) (PLGA) microspheres using oil-in-water single emulsion. Drug release profiles and degradation behaviors were monitored.

Results CDDP-Fe5 demonstrated a high initial burst (42% on day 1) and short release time (25 days) as CDDP was directly released from Fe5 nanoparticles. CDDP-Fe5 encapsulated within the PLGA microspheres revealed a lower initial burst (23% on day 1) and longer release time (55 days) than CDDP-Fe5. Compared with PLGA microspheres containing only CDDP, which showed typical biphasic release manner, microspheres with CDDP-Fe5 and CDDP demonstrated a nearly linear release after the initial burst. Fe5 and CDDP delayed microsphere degradation. All samples became porous, disintegrated, fused, and formed pellets at the end of the study.

Conclusion Fe5/PLGA composite microspheres showed favorable CDDP release behavior compared to microspheres composed of polymer alone, suggesting its potential as a new CDDP formulation.

KEY WORDS cisplatin · drug release · hydroxyapatite · microspheres · poly(lactide-*co*-glycolide)

ABBREVIATIONS

2Fe5/PT	PLGA microspheres with Fe5 nanoparticles and CDDP at feed ratio of Fe5/CDDP as 2/1 by weight
2PT-Fe5/PT	PLGA microspheres with CDDP-Fe5 and CDDP at feed ratio of CDDP-Fe5/CDDP as 2/1 by weight
CDDP	cisplatin
CDDP-Fe5	CDDP-loaded Fe5 nanoparticles
DCM	dichloromethane
DL	drug loading
DSC	differential scanning calorimeter
ED_{50}	median effective dose
Fe5	Fe^{3+} doped hydroxyapatite at atomic ratio of $Fe_{added}/Ca_{added} = 5\%$
FESEM	field emission scanning electron microscopy
FTIR	Fourier transform infrared spectroscopy
GPC	gel permeation chromatography
HA	hydroxyapatite
ICP	inductively coupled plasma
LE	loading efficiency
M_n	number-average molecular weight
M_w	weight-averaged molecular weight
O/W	oil-in-water

Electronic supplementary material The online version of this article (doi:10.1007/s11095-011-0600-9) contains supplementary material, which is available to authorized users.

Y. Li • S. Lim (✉)
Division of Bioengineering
School of Chemical and Biomedical Engineering
Nanyang Technological University
70 Nanyang Dr., Block N1.3
Singapore 637457, Singapore
e-mail: SLim@ntu.edu.sg

C. P. Ooi (✉)
School of Science and Technology SIM University
Singapore 599490, Singapore
e-mail: CPOoi@unisim.edu.sg

PBS	phosphate-buffered saline
PLGA	poly(lactide-*co*-glycolide)
PT	PLGA microspheres with only CDDP
PT-Fe5	PLGA microspheres with only CDDP-Fe5
PT-Fe5/PT	PLGA microspheres with CDDP-Fe5 and CDDP at feed ratio of CDDP-Fe5/CDDP as 1/1 by weight
PVA	poly(vinyl alcohol)
T_g	glass transition temperature
THF	tetrahydrofuran
XRD	X-ray diffraction

INTRODUCTION

Cisplatin (CDDP) is a potent anticancer drug and frequently used to treat osteosarcoma (1). Upon cellular uptake, CDDP binds to DNA and causes DNA cross linking which triggers apoptosis (2). The therapeutic activity of CDDP appears to be proportional to the intensity of single dose and the cumulative dose, however the exploitation of its full therapeutic potential has been limited by dose-dependent nephrological and neurological toxicities (3). Nephrotoxicity, which is generally irreversible, is a major cause of CDDP-associated acute and chronic morbidity and toxicity-associated mortality. While neurotoxicity is cumulative-dose dependent, the symptoms are detected only after considerable toxicity has occurred. Furthermore, *in vitro* studies have shown that CDDP has a direct effect on growth plate chondrocytes that in animals results in decreased growth rate and final height (4). Since osteosarcoma often occurs in teenagers during puberty (1), these side effects would negatively impact the patients' quality of life. In addition to the toxic effects of CDDP, the intravenous administration route is inconvenient and costly. Thus, drug carrier has been proposed for CDDP to lower the side effects and improve patients' compliance.

To date, many carriers have been fabricated for CDDP, such as nano- (5–9) and micro- (2,10–17) particles, micelles (18), liposomes (19) and insertable matrix-type device (20). Among them, microparticles have attracted great interest due to the potential for local administration, hence reduced systemic toxicity and enhanced local efficacy of chemotherapy (21). Among the previously studied nanoparticles, calcium phosphate nanoparticles, such as hydroxyapatite (HA) loaded with CDDP (9) have been suggested for osteosarcoma treatment because of the excellent biological properties of HA, which includes non-toxicity, high bioresorbability, and biocompatibility. The interaction between CDDP and HA nanoparticles is electrostatic attraction, where CDDP, a positively charged molecule is attracted to negatively charged particles like HA in aqueous phase. Hence modifying the surface properties of HA by introducing other metal ions which increases its negativity would affect the drug loading (DL). Here, iron(III) (Fe^{3+}) doped HA at atomic ratio of $Fe_{added}/Ca_{added}=0.05$ (Fe5) was synthesized using wet chemical method coupled with ion exchange mechanism to increase the drug loading capacity. Fe5 nanoparticles were observed to be elongated spheroids of ~70 nm with a small size distribution using field emission scanning electron microscopy (FESEM) and non-cytotoxic to osteoblast cells according to the *in vitro* cell studies (22). However, the release of CDDP from the surface of HA nanoparticles usually demonstrated a high initial burst (7–9). In this research, the drug-loaded nanoparticles were further encapsulated into polymer microspheres to lower the initial burst and give a controllable release since polymeric matrix would offer a diffusion barrier for CDDP. The effect of nanoparticles on the degradation of polymer and the drug release profile was also investigated.

Poly(lactide-*co*-glycolide) (PLGA) is the most commonly used polymer for CDDP in microparticulate form (11–17) due to its biocompatibility and biodegradability. The drug release from PLGA microparticles is a result of drug diffusion and polymer degradation. The degradation of PLGA is a random chain scission process, autocatalyzed by the acidic degradation products, carboxyl and hydroxyl end groups. As HA ($Ca_{10}(PO_4)_6(OH)_2$) is basic in nature, the presence of HA nanoparticles inside PLGA matrix may either catalyze the cleavage of ester bonds or neutralize the acidic degradation products and subsequently affect the degradation rate of PLGA. To date, conflicting results have been reported regarding the role of HA on the degradation of PLGA. Li *et al.* (23) reported that incorporation of HA accelerated the degradation of HA/PLGA sponge-like scaffold; while Agrawal *et al.* (24) showed that HA decreased the degradation of HA/PLGA condense implant. On the other hand, it has been speculated that the acidic degradation products may contribute to the adverse postoperative effects of the PLA-PGA implants (24,25). After 36 h of culture, death and detachment of osteoblast cells were observed on microporous poly glycolide substrate, while with the incorporation of carbonated hydroxyapatite, cell proliferation was improved (26). Hence, the incorporation of hydroxyapatite nanoparticles might have the potential to neutralize the acidic degradation byproducts, hence improved biocompatibility of the PLGA systems, and affect the polymer degradation process along with drug release.

The purpose of this study is to develop an injectable microparticulate drug delivery system composed of PLGA and hydroxyapatite nanoparticles for local release. The *in situ* delivery system was designed to release CDDP at the tumor site for a period of ~10 weeks, which is usually the period of neoadjuvant (preoperative) chemotherapy (1), in a sustained and controlled manner. Fe5 was synthesized and characterized as reported in our previous work (22). CDDP was loaded onto pure HA or Fe5 nanoparticles in aqueous

solution. The loading conditions, including temperature and shaking speed, were varied to achieve high loading. CDDP-loaded Fe5 nanoparticles (CDDP-Fe5) were then characterized using X-ray diffraction (XRD), Fourier transform infrared (FTIR) spectroscopy and FESEM. The DL was quantified using inductively coupled plasma (ICP) based on the concentration of Pt.

CDDP-Fe5 with the highest DL was encapsulated into PLGA microspheres using oil-in-water (O/W) single emulsion technique. The drug release and degradation studies were carried out in phosphate-buffered saline (PBS) solution (pH 7.4) at 37°C for 55 days. Gel permeation chromatography (GPC), differential scanning calorimeter (DSC) and FESEM were used to monitor the change in average molecular weight and glass transition temperature (T_g) of polymer, and morphology of microspheres respectively.

MATERIALS AND METHODS

Materials

CDDP (≥99.9% trace metal basis), NaH_2PO_4 and Na_2HPO_4 (≥99%, reagent plus), NaOH (≥99%, reagent grade), poly (vinyl alcohol) (PVA, 87–89% hydrolyzed), PBS (pH 7.4), tetrahydrofuran (THF, Chromasolv) were from Sigma-Aldrich. KBr (Spectrosol) and dichloromethane (DCM, 99.5%, AnalaR grade) were from BDH. HCl (37%, for analysis) was from Merck. PLGA (molar ratio of DL-lactide/glycolide as 50/50, intrinsic viscosity of 0.61 dl/g) was from Durect Corporation (Pelham, AL, USA). All chemicals were used as received or otherwise stated.

Loading of CDDP Onto Pure HA and Fe5 Nanoparticles

CDDP was dissolved in 10 mM phosphate-buffered (PB) solution (prepared from NaH_2PO_4 and Na_2HPO_4 solutions and pH was adjusted by NaOH) at 0.4 mg/ml. NaCl was omitted from the solution since Cl^- ions inhibited the binding of CDDP onto HA nanoparticles (7). Pure HA or Fe5 nanoparticles were suspended in the CDDP solution at 6.67 mg/ml. To disperse the nanoparticles, the suspension was sonicated for 10 min. The suspension was then incubated for 24 h to maximize the loading of CDDP (9) with (200 rpm) or without shaking at 25°C or 37°C. Samples were then centrifuged at 5,530×*g* for 10 min. The supernatant was discarded and the precipitate was washed once with deionized (DI) water to remove the unadsorbed species. The precipitate was dried in a vacuum oven at room temperature and ground to powder with a mortar and a pestle for further characterization.

Characterization of CDDP-Fe5

The phases present were identified using X-ray diffractometer (D8 Advanced XRD, Bruker) with Cu Kα radiation at 40 kV and 40 mA. The step size and counting time at each step were 0.04° and 10 s, respectively.

The functional groups of the powders were examined by FTIR spectroscopy (Spectrum GX, PerkinElmer). The scans were averaged over five runs at a resolution of 1 cm^{-1}. The FTIR specimens were prepared by mixing sample powder with KBr and compressing the powder into pellets at 8-ton load.

The morphology of product was observed under a FESEM (JSM-6700F, JEOL). Before observation, samples were coated with platinum at 20 mA for 100 s using a sputter (JFC-1600, JEOL).

The DL was quantified using ICP (Optima 2000, PerkinElmer) based on the concentration of Pt. ICP was calibrated using standard solutions of Pt. For measurement, 5 mg of CDDP-loaded nanoparticles was dissolved in 5 ml of 1 w/v% HCl. The DL and loading efficiency (LE) were calculated based on Eq.-s 1 and 2.

$$\text{Drug loading (\%)} = \frac{\text{weight of CDDP loaded}}{\text{weight of particles}} \times 100\% \quad (1)$$

$$\text{Loading efficiency (\%)} = \frac{\text{drug loading}}{\text{theoretical drug loading}} \times 100\% \quad (2)$$

For the analysis of DL result, zeta potential of pure HA and Fe5 in 10 mM PB solution at 6.67 mg/ml was assessed using a zetasizer system (Nano-ZS, Malvern) at 25°C and 37°C while the specific surface area was measured using BET method.

Fabrication of PLGA Microspheres

The O/W single emulsion method was modified to prepare drug loaded microspheres in Table I. Since theoretical drug loading of microspheres with only CDDP-Fe5 based on Eq. 1 was very low, excess amount of CDDP was added to increase the DL. The quantity of CDDP-Fe5 was varied to investigate the effect of hydroxyapatite phase on the degradation of PLGA. Briefly, all solids, including PLGA, were dissolved or suspended in 10 ml DCM at 400 rpm for 4 h using a magnetic stirrer. The suspension was injected into 200 ml of 1 w/v% PVA solution to be emulsified at 400 rpm for 1 h using a magnetic stirrer. The stirring speed was then lowered to 200 rpm for another 3 h to evaporate the DCM completely at room temperature in a fume hood. Once the microspheres had solidified, the pH of the emulsion was adjusted to 3.5 by adding 3.7 w/v% HCl solution to eliminate the surface-

Table I The Solids in 10 ml DCM for the Fabrication of Microspheres and the Properties of Microspheres After Solidification

Sample name	Solid in DCM (g)				Feed ratio		Property of microspheres		
	CDDP-Fe5[a]	Fe5	CDDP	P(0.61)[b]	Fe5/CDDP	Fe5/P(0.61)	DL[c] (%)	LE[d] (%)	Particle size[e] (μm)
blank	0	0	0	1.54	–	–	0	0	100 ± 24
PT	0	0	0.17	1.54	–	–	6.83 ± 0.04	68.7 ± 0.37	122 ± 34
PT-Fe5	0.38	0	0	1.54	–	1/4	0.56 ± 0.01	70.2 ± 1.53	122 ± 38
PT-Fe5/PT	0.17	0	0.17	1.54	1/1	1/9	3.59 ± 0.06	39.7 ± 0.63	134 ± 30
2PT-Fe5/PT	0.38	0	0.17	1.54	9/4	1/4	2.72 ± 0.04	33.5 ± 0.37	100 ± 34
2Fe5/PT	0	0.38	0.17	1.54	9/4	1/4	2.23 ± 0.11	27.4 ± 1.35	120 ± 40

[a] CDDP-Fe5: CDDP loaded on Fe5 nanoparticles, drug loading 4.01%

[b] P(0.61): 50/50 poly(DL-lactide-co-glycolide), with intrinsic viscosity of 0.61 dl/g

[c] DL: drug loading, $W_{drug}/W_{particle} \times 100\%$

[d] LE: loading efficiency, actual drug loading/theoretical drug loading × 100%

[e] Particle size: averaged over 200 particles using light microscope

adsorbed or unincorporated Fe5 nanoparticles. This was to confine the parameters which could influence drug release and polymer degradation. The microspheres were collected using sieves with pore size of 20 μm and 150 μm (to remove defective particles), washed with DI water and dried. The final product was stored at −20°C.

Characterization of PLGA Microspheres

The morphology and particle size of microspheres was observed using FESEM and light microscope; while the DL and LE values were determined using ICP technique. Briefly, 10 mg microspheres were dissolved in 0.5 ml DCM and 5 ml of 1 w/v% HCl was added to extract CDDP into the aqueous phase. The mixture was vortexed for 5 min and centrifuged. The upper aqueous layer was collected for ICP test. The DL and LE values were calculated according to Eq.-s 1 and 2. The extraction and measurements were done in triplicate. For structure information of microspheres, XRD were used, as described in Characterization of CDDP-Fe5 part.

Degradation and Drug Release Study

Microspheres (20 mg) were dispersed in 2 ml PBS (pH 7.4). For degradation study, 1.8 ml PBS was taken out for pH measurement and fresh PBS was refilled at predetermined time points. For characterization, samples were collected weekly, washed with DI water and dried overnight in a vacuum oven at room temperature. Samples were stored at −20°C until each characterization.

For drug release study, the 1.8 ml PBS solution was stabilized in 1 w/v% HCl at a volumetric ratio of 1/1 for ICP test. The CDDP release was calculated in terms of cumulative release (% w/w). To verify the repeatability of the drug release, all the release tests were carried out in triplicate.

Characterization of Degraded Microspheres

The change in molecular weight and glass transition temperature T_g, of polymer were monitored using GPC (LC-20AD, Shimadzu) and DSC (Diamond DSC, Perkin Elmer), respectively. The morphology of microspheres was observed under FESEM.

Average molecular weight and polydispersity index (PI) of samples were determined using a Shimadzu LC-20AD instrument equipped with a PLgel GPC column and a RID-10A refractive index detector. The system was calibrated using a series of polystyrene standards with weight-averaged molecular weight (M_w) ranging from 500 kDa to 162 Da. The mobile phase was THF at a flow rate of 1 ml/min at 40°C. Samples were dissolved in THF at 2 mg/ml, filtered and filled into 2 ml vials. The solution was then injected into the column using auto sampling function. The degradation rate constant could be obtained based on the degradation mechanism (27), where the number-average molecular weight (M_n) of PLGA followed Eq. 3 in the early stage of degradation process:

$$\ln M_n = \ln M_{n,0} - k_{Mn} t \tag{3}$$

where $M_{n,0}$ is the number-average molecular weight of polymer before degradation and k_{Mn} is the rate constant of the degradation process.

T_g was quantified to assess the mobility of polymer chains along with degradation. After equilibrating at −20°C for 5 min, samples were heated up to 100°C at a rate of 10°C/min under nitrogen atmosphere. T_g was determined as the onset temperature of glass transition from the DSC heating thermograph.

Table II Drug Loading (DL) and Loading Efficiency (LE) of CDDP on Pure HA and Fe5 at Different Loading Conditions. The Concentration of CDDP was 0.4 mg/ml in 10 mM Phosphate-Buffered Solution at pH 7.4 and free of Cl^-

Shaking speed[a] (rpm)	T (°C)	Pure HA		Fe5	
		DL (%)	LE (%)	DL (%)	LE (%)
200	25	1.37	22.8	2.85	47.5
0	25	1.05	17.5	2.54	42.3
200	37	2.55	42.5	4.01	66.8
0	37	1.89	31.5	3.36	56.0

[a] shaking speed, controlled by a benchtop incubator shaker (Excella E24, New Brunswick Scientific)

RESULTS

Loading of CDDP on Hydroxyapatite Nanoparticles

Drug loading was measured using ICP based on Pt concentration. As shown in Table II, the DL and LE values for both pure HA and Fe5 at shaking speed of 200 rpm were higher than at 0 rpm when the temperature was kept constant. In the case of fixed shaking speed, the DL and LE values at 37°C were higher than the values at 25°C. Under the same loading conditions, the DL and LE values for Fe5 were higher than those for pure HA. Thus, CDDP-Fe5, fabricated at shaking speed of 200 rpm at 37°C, was chosen for further studies. Under this condition, the DL value of Fe5 was 4.01%, which was 57% higher than pure HA.

Zeta potential and specific surface area of pure HA and Fe5 were measured for the interpretation of drug loading results. As shown in Table III, the magnitude of zeta potential for both samples at 37°C was slightly higher than at 25°C. Fe5 nanoparticles were more negatively charged than pure HA regardless of temperature. Since Fe5 was synthesized using ion exchange method, the nanoparticles morphology and size were similar to pure HA. Its specific surface area was also similar to pure HA within experimental error (Table III). The presence of Fe^{3+} ions in Fe5 increased the negative charge of the nanoparticles, which attracted larger quantity of positively charged CDDP species and resulted in higher DL values than pure HA.

Characterization of CDDP-Fe5

The structure and morphology of CDDP-Fe5 was studied by XRD, FITR and FESEM. The XRD peaks of as-received CDDP were sharp and narrow, indicating that the drug was highly crystalline (Fig. 1). For CDDP-Fe5, only peaks belonging to hydroxyapatite phase were present. This suggested that CDDP was not crystalline in CDDP-Fe5, thus no peaks corresponding to CDDP were observed in the XRD pattern. The presence of CDDP in CDDP-Fe5 was confirmed by ICP result as shown in Table II. Compared to Fe5, no peak broadening or shift was observed for CDDP-Fe5 due to the loading of CDDP. In the FTIR spectra of as-received CDDP, the characteristic NH_3 absorption bands (28) were present, such as the stretching bands (3,274, 3,188 cm^{-1}), asymmetric deformation modes (1,618, 1,534 cm^{-1}), skeletal deformation mode (1,304, 1,298 cm^{-1}) and in phase rocking mode (797 cm^{-1}). For CDDP-Fe5, only the stretching bands of NH_3 at around 3,300 cm^{-1} and skeletal deformation bands at around 1,300 cm^{-1} were observed (indicated by arrows). This was probably because of the low CDDP loading and/or bands overlap. The FESEM image of CDDP-Fe5 showed that the nanoparticles were elongated spheroids similar to Fe5 and the size was not affected by CDDP adsorption, still ~70 nm (Fig. 1). None of the large crystallite of as-received CDDP was observed in the FESEM image of CDDP-Fe5.

Characterization of Microspheres Before Degradation

The modified O/W single emulsion method was used to fabricate the PLGA microspheres. As shown in Table I, the particle size was similar for all samples within experimental error, which was around 110 μm. The sample with only CDDP encapsulated into PLGA microspheres (PT) had the

Table III Zeta Potential of Pure HA and Fe5 Powder in 10 mM Phosphate-Buffered Solution (pH 7.4, free of Cl^-) at 25°C and 37°C and their Specific Surface Area from BET Data

Sample name	Zeta potential (mV)		Specific surface area (m^2/g)
	25°C	37°C	
pure HA	−29.5 ± 0.9	−26.7 ± 2.2	90 ± 18
Fe5	−36.7 ± 1.0	−35.7 ± 1.5	92 ± 15

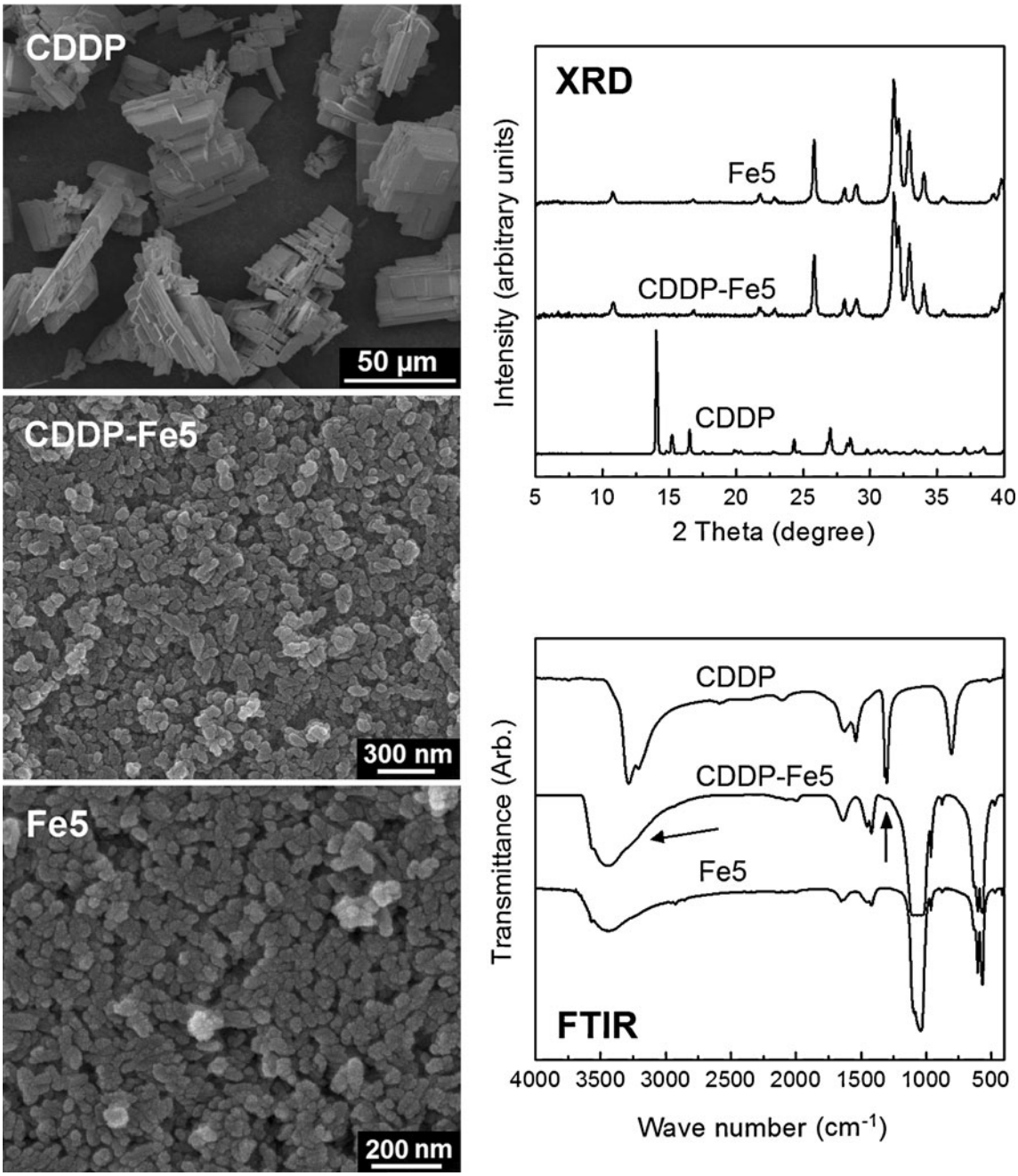

Fig. 1 Characterization of CDDP-Fe5 using FESEM, XRD, and FTIR.

highest DL of 6.83% while microspheres with only CDDP-Fe5 (PT-Fe5) had the lowest DL of 0.6% but the highest LE value. The presence of Fe5 nanoparticles appeared to have a negative effect on the DL and LE values. As shown in Table I, for samples PT, PT-Fe5/PT and 2PT-Fe5/PT, the DL and LE values decreased with the increase of CDDP-Fe5. For sample 2Fe5/PT, the DL and LE values were also much smaller than PT. The negative effect of Fe5 on drug loading of microspheres may be due to its hydrophilicity which facilitated the diffusion of drug into the surrounding water phase during solidification of the microspheres.

The structure information of microspheres was obtained using XRD while the morphology was observed under FESEM. The as-received CDDP was a crystalline powder and remained crystalline in the PLGA microspheres. As shown in Fig. 2, the XRD patterns of microspheres had sharp peaks corresponding to CDDP. The position and width of Fe5 peaks (Fig. 2c) did not change significantly after the nanoparticles entrapped in

the microspheres compared to CDDP-Fe5 (Fig. 2d). In addition, the broad peak of PLGA at around 20° was observed in all microspheres.

As shown in Fig. 3, all microspheres were spherical but with different surface morphologies. The blank and PT samples, without Fe5, had smooth surfaces without pores. For those with Fe5 nanoparticles, the surface was wrinkled and some pores were observed.

Degradation of Microspheres

The change in molecular weight of polymer was monitored using GPC. As shown in Fig. 4a, M_n decreased upon incubation in PBS to the endpoint of study, 55th day. After immersion of microspheres in aqueous phase, water molecules penetrated into the polymer matrix and cleavage of ester bonds began. M_n appeared to decrease at a slower rate after 28 days of degradation. Based on Eq. 3, the degradation rate constants for all samples were calculated from the slope of the linear regression fit on logarithm of M_n (between 0 and 49 days). The k_{Mn} values for all samples are listed in Table IV. The values decreased due to the presence of CDDP and/or Fe5, indicating that CDDP and/or Fe5 slowed down the degradation rate of PLGA.

The change in the distribution of molecular weight was reflected by PI, which increased up to 28 days and decreased thereafter until the 55th day (Fig. 4b). The pattern was similar to Chen's result (29), where PI values

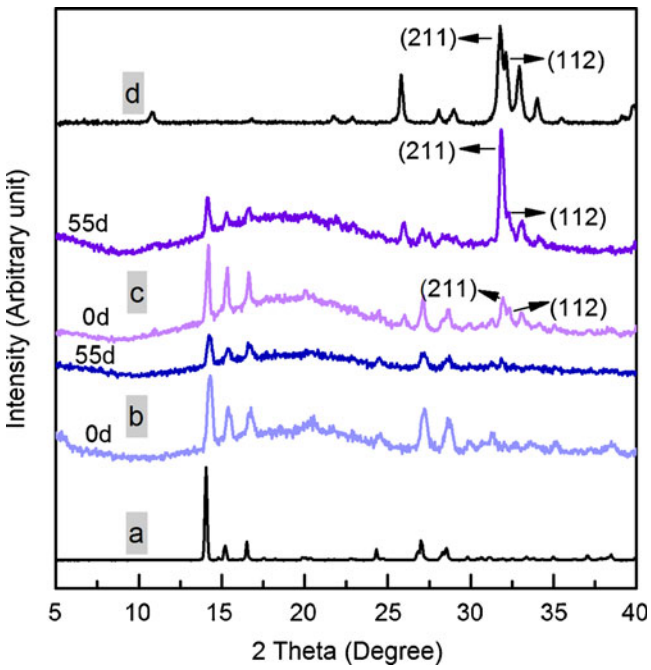

Fig. 2 The representative XRD patterns of (**a**) as-received CDDP, (**b**) PT, and (**c**) PT-Fe5/PT before degradation and incubated in PBS for 55 days, and (**d**) CDDP-Fe5.

increased initially (up to 13th week) and eventually decreased at longer degradation time (22 weeks). The initial increment of PI value was due to the random cleavage of ester bonds which decreased the molecular weight of the polymer and broadened its distribution. As degradation continued, the degradation byproducts of lower molecular weight at ~1,100 Da (30) were released into the surrounding solution thus decreasing the PI value. The PI of blank sample reached the maximum value earliest and PT-Fe5 and PT-Fe5/PT reached the peak value latest among samples (Fig. 4b).

T_g is an important parameter to assess the mobility of polymer chains and was determined using DSC. As shown in Fig. 5, T_g increased initially and then decreased at longer degradation time. The changed trend of T_g values was possibly due to structural relaxation which would increase T_g (31) and polymer degradation which decreased polymer molecular weight and thus T_g according to Fox-Flory equation (32).

Since lactic acid and glycolic acid were reported to be detected in the solution after 1-day incubation of PLGA microspheres (33), the pH of PBS solution was monitored during the degradation process. It remained around 7.4 for the first 20 days, followed by a sharp decrease with further degradation and eventually stabilized, as shown in Fig. 6. The sharp decrease in the pH values were fitted using linear regression ($pH = -k_{pH} \times Time + const$) and tabulated in Table IV. The commencement time of the second pH stabilization phase was after 40 days, irrespective of the samples. For samples with Fe5, the pH values at around 50th day were higher than samples without Fe5. This was possibly due to the neutralization of the acidic degradation products by the Fe5 nanoparticles which subsequently lowered the polymer degradation rate.

The morphology of microspheres at different degradation time was observed under FESEM. In the first 21 days, there were no significant changes (Fig. 3), where all samples were spherical. On the 14th day, small pores of around 100 nm were observed on microspheres surface for all samples (Supplementary Material). On the 21st day, sample 2Fe5/PT was swollen as some particles were much larger than 150 μm (the maximum size for all samples as described in "Fabrication of PLGA Microspheres").

After 28 days, the morphological change was obvious, where for samples without Fe5, blank and PT, the microspheres surface became wrinkled (Fig. 3) and the sponge-like internal structure was observed (Supplementary Material). For the other samples with Fe5, the surface of microspheres was much smoother and the surface pores were much smaller. Partial particles of 2Fe5/PT were disintegrated and the porous interior was observed.

On the 35th day, all particles of 2Fe5/PT and a portion of the particles in other samples were observed to be

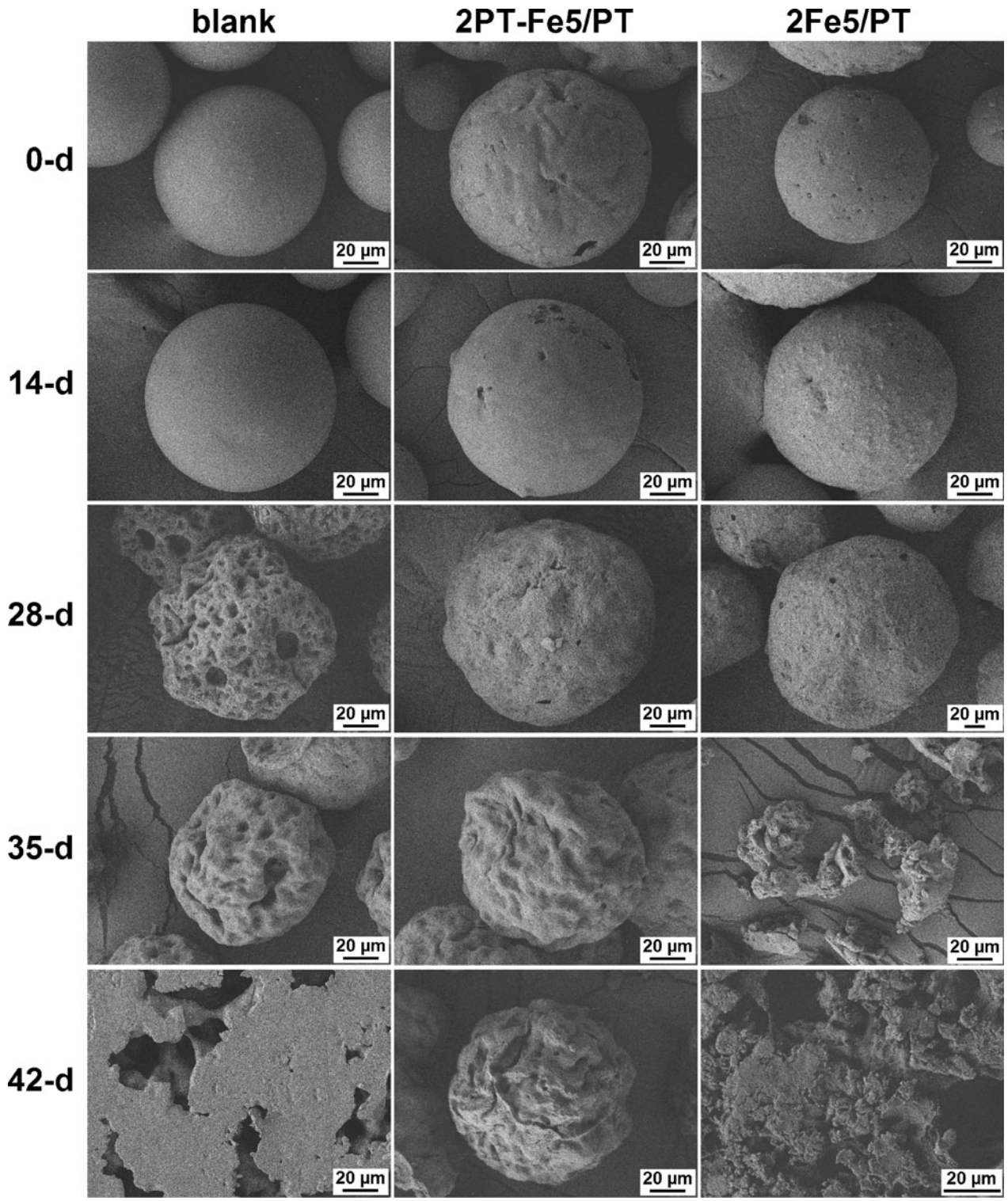

Fig. 3 Representative FESEM image of microspheres blank, 2PT-Fe5/PT and 2Fe5/PT before degradation and at different degradation times, day 14, 28, 35, and 42.

disintegrated. For blank and PT, microspheres surface was still wrinkled while for PT-Fe5, PT-Fe5/PT and 2PT-Fe5/PT, the surface of microspheres became rougher than on the 28th day. The size of pores on all microspheres appeared to decrease when compared with the 28th day (Supplementary Material). After 42 days, all samples, except for PT-Fe5 and 2PT-Fe5/PT, were completely disintegrated while for blank sample, the polymer had

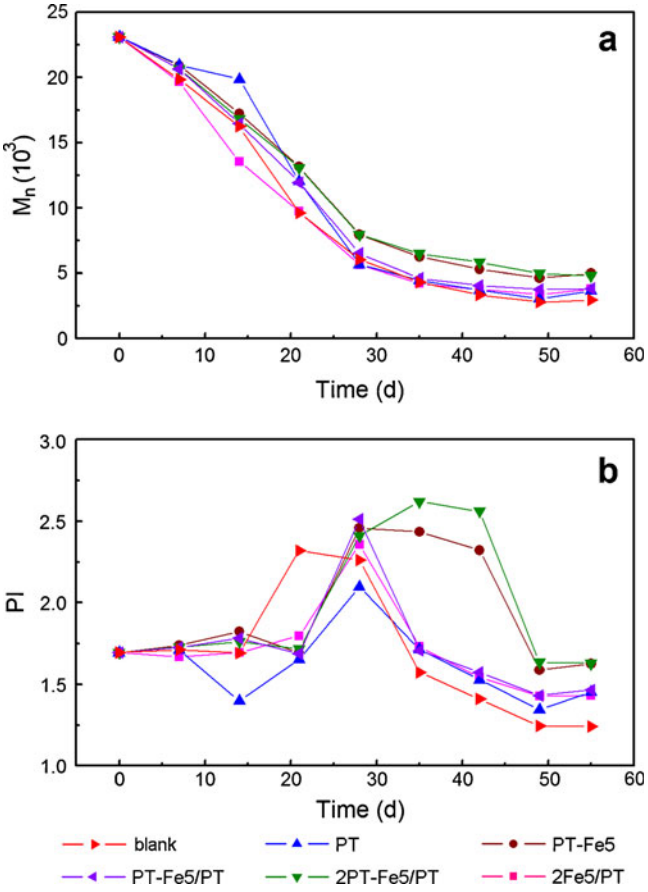

Fig. 4 (**a**) The number-average molecular weight (M_n) and (**b**) the polydispersity index (PI) of all samples as a function of degradation time.

fused to form pellets. On the 49th day, only PT-Fe5 had some entire particles. At the end of degradation study, the 55th day, all samples had disintegrated and fused to form insoluble pellets. The morphology was similar to the blank sample on the 42nd day (data not shown).

In summary, small pores were formed on the microspheres surface after degradation for 14 days, which gradually enlarged and increased in number with further degradation until 28 days, and then the pores were observed to be smaller and less on 35th day. As degradation proceeded, the surface of microspheres became rougher gradually, which was followed by the disintegration of microspheres structure.

Table IV The Degradation Rate Constant k_{Mn} and Decreasing Rate of pH Values k_{pH} for all Samples

Sample	M_n		pH	
	k_{Mn}	R^2	k_{pH}	R^2
blank	0.1121	0.9939	0.0477	0.9786
PT	0.0905	0.9773	0.0455	0.9654
PT-Fe5	0.0348	0.9843	0.0367	0.9707
PT-Fe5/PT	0.066	0.9848	0.0428	0.9566
2PT-Fe5/PT	0.035	0.9845	0.0346	0.9687
2Fe5/PT	0.0494	0.9821	0.0438	0.9661

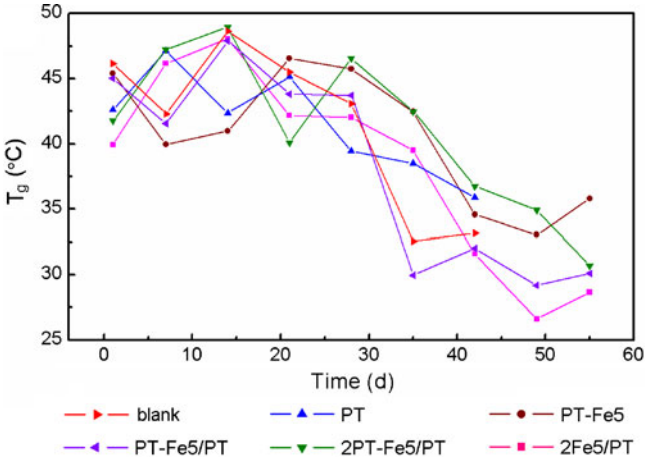

Fig. 5 The glass transition temperature (T_g) of all microspheres as a function of degradation time.

Drug Release from Microspheres

Fractional cumulative CDDP release is shown in Fig. 7. For CDDP-Fe5, a high initial burst (41.8%) on the 1st day was observed, followed by a continuous release for 25 days (Fig. 7a). The profile was similar to Palazzo's result (9). On the other hand, CDDP-Fe5 entrapped in PLGA micro-

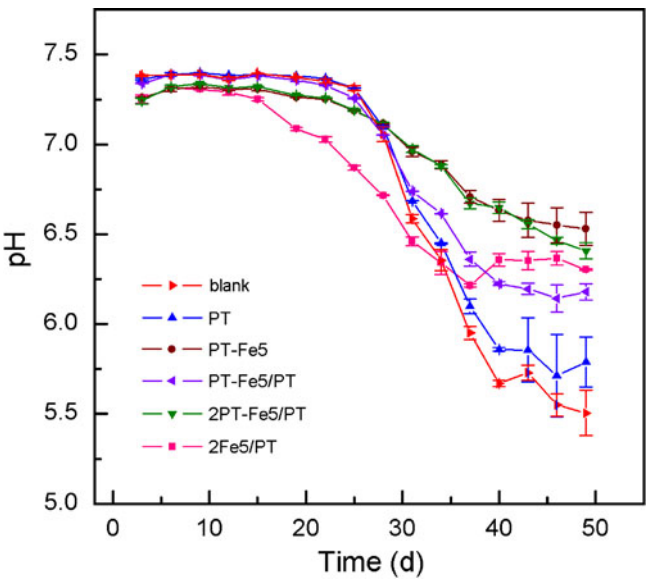

Fig. 6 The pH values of PBS solution for all microspheres as a function of degradation time.

spheres (PT-Fe5; Fig. 7b), showed a lower initial burst with longer release time (55 days). The drug release of sample PT followed a typical biphasic manner (Fig. 7e), where the initial burst and induction period lasted for 23 days, followed by a final burst release (1.58%/day). For PT-Fe5/PT, the release pattern (Fig. 7f) was similar to PT (Fig. 7e) for the initial 25 days and after 25 days, it appeared to be linear. In the case of 2PT-Fe5/PT, the release profile was nearly linear after the initial burst (Fig. 7d) while the release rate was slower than PT-Fe5. For sample 2Fe5/PT, the release profile (Fig. 7c) was similar to PT-Fe5 after 15 days. For the first 15 days, the release rate of 2Fe5/PT (Fig. 7c) was slower than PT-Fe5 (Fig. 7b).

As compared with CDDP-Fe5, the initial burst of PT-Fe5 was much lower. The result was expected as the absence of diffusion barrier like polymer matrix resulted in release of CDDP directly from the nanoparticles into the surrounding media. For samples at high Fe5 feed ratio (Fe5/PLGA = 1/4), ~23% of the total drug was released during the initial burst stage, which was higher than samples with lower and no Fe5, PT-Fe5/PT and PT (~10%) (Fig. 7). This might be due to the hydrophilicity of Fe5 which attracted water and increased mobility of polymer chains, hence facilitated drug diffusion.

The median effective dose (ED_{50}) (the dose which is pharmacologically effective for 50% of the population exposed to the drug) of CDDP has been reported to be 0.35–1.4 μg/ml *in vitro* (34). Since different samples had different drug loading and all samples were incubated in 2 ml PBS for drug release study, different initial concentrations of microspheres are required to ensure that the CDDP concentrations fall within the therapeutic range. For CDDP-Fe5, the concentrations of CDDP fell within the ED_{50} range between the 12th and 25th day, which were 0.35–0.95 μg/ml and lasted for 14 days (Fig. 8a). This range could be achieved at CDDP-Fe5 concentration of 1.35 mg/ml. Once CDDP-Fe5 entrapped inside polymer microspheres (PT-Fe5), the release rate became more controllable (Fig. 8a). The concentrations in the ED_{50} range were from the 9th to 55th day with the exception of 19th to 25th day. The values were between 0.35 and 0.89 μg/ml and could be obtained at PT-Fe5 concentration of 8.77 mg/ml. The CDDP concentrations within the ED_{50} range lasted for 37 days, which was much longer than 14 days for CDDP-Fe5.

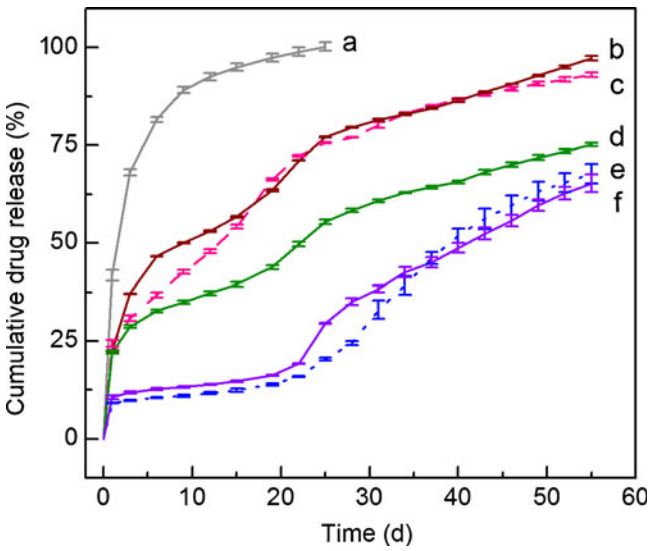

Fig. 7 Fractional cumulative release of CDDP from (**a**) CDDP-Fe5 and microspheres, (**b**) PT-Fe5, (**c**) 2Fe5/PT, (**d**) 2PT-Fe5/PT, (**e**) PT, (**f**) PT-Fe5/PT in 10 mM PBS (pH 7.4) at 37°C. Data = mean ± standard deviation; n = 3.

For sample PT, the CDDP concentrations from the 3rd to 19th day were in the ED_{50} range of CDDP (Fig. 8b), which were 0.35–1.19 μg/ml and could be achieved at PT concentration of 2.32 mg/ml. During this period, diffusion dominated the drug release. Beyond this time frame, the concentrations of CDDP were much higher than the therapeutic range, where it reached the maximum value on the 31st day and gradually decreased afterwards. In the case of PT-Fe5/PT, the concentrations of diffusion release from the 3rd to 19th day were below the therapeutic range. After diffusion stage, the concentration reached maximum value on the 25th day and maintained ~0.50 μg/ml with further drug release time. This period lasted from 28th to 55th day, during which the concentrations fell within the range of 0.35–0.78 μg/ml and were within the therapeutic range of CDDP. This concentration range could be obtained at PT-Fe5/PT concentration of 0.79 mg/ml. When compared with PT-Fe5/PT, a shorter time range (17 days) was applicable for sample PT during the drug release study.

For 2PT-Fe5/PT, the concentrations at various time intervals in the ED_{50} range were 0.35–1.09 μg/ml from the 6th to 19th day and 0.35–0.75 μg/ml from the 28th to 55th day (Fig. 8c). This would be obtained at 2PT-Fe5/PT concentration of 1.89 mg/ml. The CDDP concentrations within ED_{50} range nearly lasted the entire drug release period, 55 days except for the initial burst release and the 2nd burst release period. The time range (~48 days) was longer than PT-Fe5. For 2Fe5/PT, the CDDP concentrations fell within ED_{50} range during the later stage of drug release, from the 25th to 55th day. The values were between 0.35 μg/ml and 1.03 μg/ml and could be achieved at 2Fe5/PT concentration of 2.81 mg/ml. The period within ED_{50} range was shorter than 2PT-Fe5/PT as shown in Fig. 8c.

Based on the comparison, it was found the microspheres at feed ratio of Fe5/PLGA of 1/4 had more controllable CDDP concentrations at various time intervals than microspheres with less or no Fe5 and also free CDDP-Fe5 without polymer

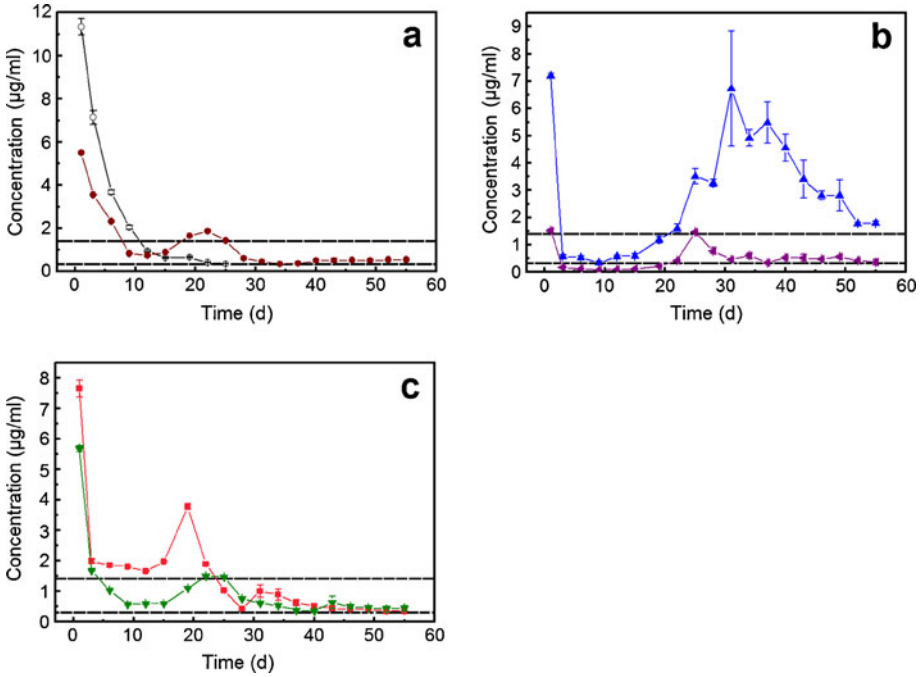

Fig. 8 CDDP concentrations of (**a**) CDDP-Fe5 (○) and PT-Fe5 (●), (**b**) PT (▲) and PT-Fe5/PT (◀), (**c**) 2PT-Fe5/PT (▼) and 2Fe5/PT (■) at various time intervals. Data = mean ± standard deviation; n = 3. The dash lines correspond to 0.35 μg/ml and 1.4 μg/ml respectively.

encapsulation. Among the three samples at feed ratio of Fe5/PLGA of 1/4, 2PT-Fe5/PT had the longest release time with drug concentrations within the ED_{50} range of CDDP.

At the end of study, 55th day, only 3 samples had cumulative drug release of higher than 90% while ~25% drug remained in the matrix of the other three samples (Fig. 7). The presence of CDDP and Fe5 were confirmed using XRD analysis (Fig. 2).

DISCUSSION

CDDP-Fe5

CDDP was loaded onto the surface of hydroxyapatite nanoparticles by electrostatic attraction. In aqueous phase, CDDP is hydrolyzed to be positively charged species, as shown in Eq.-s 4 and 5 (35,36). The charged species were adsorbed onto the negatively charged nanoparticles.

$$(NH_3)_2PtCl_2 + H_2O \rightleftharpoons (NH_3)_2PtCl(H_2O)^+ + Cl^- \quad (4)$$

$$(NH_3)_2PtCl(H_2O)^+ + H_2O \rightleftharpoons (NH_3)_2Pt(H_2O)_2^{2+} + Cl^- \quad (5)$$

The adsorption process is well described mathematically by the Freundlich isotherm (7,8), as shown in Eq. 6:

$$Q = kC^m \quad (6)$$

where Q is the amount adsorbed (mg/g), C is the equilibrium concentration (mg/l) of adsorbate (37,38) which is charged CDDP species in this research, k and m are constants reflecting adsorption affinity and capacity. As shown in Eq.-s 4 and 5, the charged species are produced by these endothermic equilibrated hydrolysis reactions (39). At higher temperatures, more charged species will be produced, giving rise to higher equilibrium concentration, C, in the Freundlich isotherm (Eq. 6). Hence, all samples had higher DL at 37°C (Table II), even though the zeta potential values were slightly smaller at 37°C than at 25°C (Table III).

The available adsorption sites for the same sample would be different between non-agitated and agitated samples. Agitation dispersed the nanoparticles into smaller aggregates which resulted in more exposed active sites for surface adsorption compared to samples prepared without agitation. Hence, all samples displayed higher drug loading at 200 rpm than those without agitation (Table II). Doping of HA with iron at 5% atomic ratio (Fe5) increased DL and LE values. This was probably due to the higher adsorption affinity for Fe5 in the Freundlich isotherm, which is reflected by the larger magnitude of zeta potential than pure HA. The higher DL and LE values of Fe5 than pure HA were not contributed by the surface area as the specific surface area of Fe5 was close to that of pure HA (Table III). Since CDDP was loaded onto Fe5 by surface adsorption, the structure of Fe5 was not significantly influenced.

Fabrication of PLGA Microspheres

CDDP-Fe5 and/or CDDP were encapsulated into PLGA microspheres using O/W single emulsion. The presence of

Fe5 affected the surface morphology of the microspheres (Fig. 3). This may be due to its water insolubility and hydrophilicity which influenced the solidification process. As compared with the oil droplets just after emulsion, these solid microspheres were shrunken in nature due to the loss of organic solvent (40). During solvent elimination, the encapsulated substances were partially expelled. Fe5 nanoparticles, initially in the oil droplets, might be partially stabilized in the interfacial layer between the oil phase and aqueous phase. This was similar to the results as reported by Nagata *et al.* (41), where microspheres formed without surfactant however with hydroxyapatite nanoparticles precipitated at the oil/aqueous interface as stabilizer during the solidification process. The nanoparticles were formed by co-precipitation from calcium nitrate and ammonium hydrogen phosphate in the aqueous phase. Since Fe5 was not soluble in water, the presence of Fe5 at the interfacial layer may affect the shrinkage process when the oil droplets solidified. Thus the surface of microspheres had a wrinkled texture.

Besides affecting the surface morphology, the presence of Fe5 also decreased drug loading of microspheres (Table I). It was reported that during the elimination of DCM, a gel-like layer would form on the surface of oil droplets (40). The presence of hydrophilic Fe5 nanoparticles in the gel-like layer may offer a diffuse channel for CDDP. Since CDDP is slightly soluble in aqueous solution (2.53 mg/ml at 25°C) (36), the drug loading of microspheres then decreased.

Degradation of PLGA Microspheres

The presence of Fe5 and/or CDDP delayed the polymer degradation (Table IV). The hydrolysis of PLGA is catalyzed by the acidic degradation byproducts, giving rise to autocatalysis effect. As reported by Siepmann *et al.* (42) and Klose *et al.* (43), even very small-sized microspheres (<20 μm) were affected by the autocatalysis effect. Here, the microspheres investigated were around 110 μm and thus the degradation was autocatalyzed. Fe5 (Fe^{3+} doped hydroxyapatite ($Ca_{10}(PO_4)_6(OH)_2$)) is basic in nature. Basic material has two opposite effects on PLGA degradation (44). It can either catalyze the cleavage of ester bonds, thus enhancing the degradation or it can neutralize the acidic degradation products and suppress the autocatalysis effect, resulting in lower degradation rate. Here all samples with Fe5 had smaller degradation rate constant k_{Mn} than the blank sample (Table IV). The results suggested that the neutralization of the acidic PLGA degradation byproducts by Fe5 may take precedence over the catalysis effect of Fe5 on the cleavage of ester bonds.

Besides Fe5, it was also found that CDDP decreased the degradation rate of PLGA (Table IV). The interaction between CDDP and the acidic degradation byproducts of PLGA was probably a complexation effect (Supplementary Material), which has been used to entrap CDDP in micelles (6,45) or fabricate CDDP conjugate (46). The acidic end groups were thus shielded and the autocatalysis effect was inhibited.

Since Fe5 has the potential to neutralize the acidic degradation byproducts, the pH value of PBS solution was monitored during the degradation study. After ~25 days of incubation, the pH showed a sharp decrease. Based on how fast the pH values decreased, samples were sorted according to k_{pH} values from the largest to the smallest. The trend was similar to the sequence of samples based on the degradation rate constant, k_{Mn}. The only difference was that k_{pH} of 2Fe5/PT was smaller than the value for PT-Fe5/PT while the degradation rate constant, k_{Mn} of 2Fe5/PT was larger than PT-Fe5/PT. The higher Fe5 quantity in 2Fe5/PT might contribute to the observation since Fe5 would neutralize the acidic degradation byproducts. Similarly, sample PT-Fe5 had larger degradation rate constant k_{Mn} than 2PT-Fe5/PT while their k_{pH} values were close, which was also probably due to the neutralization effect of Fe5. Here, the results were consistent with published data that hydroxyapatite neutralized the acidic degradation byproducts of PLGA or PGA and resulted in higher pH values than samples without hydroxyapatite (23,24,26).

The change in microspheres morphology was observed to correlate with the change in glass transition temperature T_g. Formation of small voids in microspheres in the first 14 days (Supplementary Material) allowed for more polymer chain movement and led to T_g decrease (Fig. 5). The high mobility of polymer chains in rubber state (T_g close to degradation temperature, 37°C, Fig. 5) also resulted in diminishing pores (Supplementary Material) in longer incubation period. This was consistent with Bouissou's result (47). Microspheres containing model protein FIII9′-10 and surfactant Triton X-100 stored at relative humidity 75% for 24 h at 20°C demonstrated reduction of surface pore depth because of the high mobility of polymer chains in rubber state. The smaller pore size after 35 days of degradation may also reduce the release rate of the water soluble acidic degradation byproducts, stabilizing the pH of the surrounding media (Fig. 6).

The morphological changes of microspheres also confirmed that the presence of Fe5 delayed the polymer degradation. Microspheres were still observed for samples PT-Fe5 and 2PT-Fe5/PT while samples free of Fe5 were completely disintegrated by 42 days of degradation (Fig. 3).

The different degradation behavior between 2PT-Fe5/PT and 2Fe5/PT was possibly due to the difference in the composition, where 2PT-Fe5/PT contained CDDP-Fe5 while 2Fe5/PT contained Fe5. Among all samples, 2Fe5/PT was the first to be observed with disintegrated particles during degradation (~28th day) even though the degradation rate constant k_{Mn} of 2Fe5/PT was smaller than the blank and PT

(Table IV). This was possible due to the weak bonding of different substances inside 2Fe5/PT microspheres, thus water molecules could easily diffuse through the polymer matrix of 2Fe5/PT before and after disintegration, and then both autocatalysis and inhibitory effects of Fe5 on autocatalysis declined. As compared to samples free of Fe5, the presence of Fe5 in 2Fe5/PT consistently delayed the polymer degradation as reflected by the smaller k_{Mn} value (Table IV).

Drug Release of PLGA Microspheres

As for drug release, due to the introduction of polymer matrix as a diffusion barrier, PT-Fe5 had a slower and more controllable release rate than CDDP-Fe5. The CDDP concentrations at various time intervals could be within the ED_{50} range for 37 days (Fig. 8a), which was much longer than 14 days for CDDP-Fe5. PT microspheres, with only CDDP, demonstrate a typical biphasic cumulative release pattern. Co-encapsulation of Fe5 nanoparticles into microspheres resulted in a more linear release profile. For sample with CDDP and CDDP-Fe5 at feed ratio of Fe5/PLGA as 1/4, 2PT-Fe5/PT, the release profile was nearly linear after the initial burst stage. This sample also had the most stable CDDP concentrations at various time intervals and the concentrations could be within the ED_{50} range of CDDP for ~48 days. This was ideal for the treatment of osteosarcoma as the chemotherapy for osteosarcoma usually lasts ~10 weeks to several months (1). A preincubation step to decrease the initial burst would be necessary in the actual drug formulation.

The controllable drug release of Fe5/PLGA composite microspheres might be a balance of the following effects. Hydrophilicity of Fe5 nanoparticles facilitated the drug diffusion. On the other hand, Fe5 also delayed polymer degradation which might slow drug release. Although Fe5 decreased the LE values of CDDP in microspheres, its effect on drug release profile was significantly favorable.

CONCLUSION

Fe5 had much higher drug loading than pure HA (57% higher) due to the possible higher affinity with CDDP. Since CDDP was surface adsorbed onto Fe5 nanoparticles, the morphology and structure of Fe5 were not significantly modified.

CDDP and CDDP-Fe5 were encapsulated into PLGA microspheres using O/W single emulsion. Both were still in crystalline state which was not affected by the fabrication process. Microspheres with Fe5 had wrinkled surface with defective pores compared with the smooth surface of samples free of Fe5. The presence of Fe5 and CDDP decreased the degradation rate of PLGA. The neutralization of the acidic degradation byproducts by the basic Fe5 appeared to be more dominant over the catalysis of Fe5 on polymer chain scission. The autocatalysis of PLGA was inhibited and the degradation rate was thus lowered. CDDP would form complex structure with the acidic degradation byproducts, hence also diminishing the autocatalysis effect. The alkaline property of Fe5 also resulted in the lower rate of the pH values of buffer solution decreasing with respect to degradation time.

The CDDP release profile of the microspheres was markedly modified by the presence of Fe5 nanoparticles. The typical biphasic release pattern could be linear when both CDDP and CDDP-Fe5 at feed ratio of Fe5/PLGA as 1/4 were entrapped in microspheres (2PT-Fe5/PT). Among all sample investigated, 2PT-Fe5/PT had the longest release period during which CDDP concentrations at various time intervals could be maintained within the ED_{50} range of CDDP.

ACKNOWLEDGMENTS & DISCLOSURES

The authors thank School of Chemical and Biomedical Engineering at Nanyang Technological University, Singapore, for funding support.

REFERENCES

1. Longhi A, Errani C, De Paolis M, Mercuri M, Bacci G. Primary bone osteosarcoma in the pediatric age: State of the art. Cancer Treat Rev. 2006;32:423–36.
2. Yanand X, Gemeinhart RA. Cisplatin delivery from poly(acrylic acid-*co*-methyl methacrylate) microparticles. J Control Release. 2005;106:198–208.
3. Cvitkovic E. Cumulative toxicities from cisplatin therapy and current cytoprotective measures. Cancer Treat Rev. 1998;24:265–81.
4. van Leeuwen BL, Kamps WA, Jansen HWB, Hoekstra HJ. The effect of chemotherapy on the growing skeleton. Cancer Treat Rev. 2000;26:363–76.
5. Avgoustakis K, Beletsi A, Panagi Z, Klepetsanis P, Karydas AG, Ithakissios DS. PLGA-mPEG nanoparticles of cisplatin: *in vitro* nanoparticle degradation, *in vitro* drug release and *in vivo* drug residence in blood properties. J Control Release. 2002;79:123–35.
6. Jeong Y-I, Kim S-T, Jin S-G, Ryu H-H, Jin Y-H, Jung T-Y, *et al.* Cisplatin-incorporated hyaluronic acid nanoparticles based on ion-complex formation. J Pharm Sci. 2008;97:1268–76.
7. Barroug A, Glimcher MJ. Hydroxyapatite crystals as a local delivery system for cisplatin: adsorption and release of cisplatin *in vitro*. J Orthop Res. 2002;20:274–80.
8. Barroug A, Kuhn LT, Gerstenfeld LC, Glimcher MJ. Interactions of cisplatin with calcium phosphate nanoparticles: *In vitro* controlled adsorption and release. J Orthop Res. 2004;22:703–8.
9. Palazzo B, Iafisco M, Laforgia M, Margiotta N, Natile G, Bianchi CL, *et al.* Biomimetic hydroxyapatite-drug nanocrystals as potential bone substitutes with antitumor drug delivery properties. Adv Funct Mater. 2007;17:2180–8.

10. Ike O, Shimizu Y, Wada R, Hyon SH, Ikada Y. Controlled cisplatin delivery system using poly(d, l-lactic acid). Biomaterials. 1992;13:230–4.
11. Fujiyama J, Nakase Y, Osaki K, Sakakura C, Yamagishi H, Hagiwara A. Cisplatin incorporated in microspheres: development and fundamental studies for its clinical application. J Control Release. 2003;89:397–408.
12. Matsumoto A, Matsukawa Y, Horikiri Y, Suzuki T. Rupture and drug release characteristics of multi-reservoir type microspheres with poly(dl-lactide-*co*-glycolide) and poly(dl-lactide). Int J Pharm. 2006;327:110–6.
13. Matsumoto A, Matsukawa Y, Suzuki T, Yoshino H. Drug release characteristics of multi-reservoir type microspheres with poly(dl-lactide-*co*-glycolide) and poly(dl-lactide). J Control Release. 2005;106:172–80.
14. Matsumoto A, Matsukawa Y, Suzuki T, Yoshino H, Kobayashi M. The polymer-alloys method as a new preparation method of biodegradable microspheres: principle and application to cisplatin-loaded microspheres. J Control Release. 1997;48: 19–27.
15. Itoi K, Tabata CY, Ike O, Shimizu Y, Kuwabara M, Kyo M, *et al.* *In vivo* suppressive effects of copoly(glycolic/L-lactic acid) microspheres containing CDDP on murine tumor cells. J Control Release. 1996;42:175–84.
16. Huo D, Deng S, Li L, Ji J. Studies on the poly(lactic-*co*-glycolic) acid microspheres of cisplatin for lung-targeting. Int J Pharm. 2005;289:63–7.
17. Moreno D, de Ilarduya CT, Bandre E, Bunuales M, Azcona M, Garcia-Foncillas J, *et al.* Characterization of cisplatin cytotoxicity delivered from PLGA-systems. Eur J Pharm Biopharm. 2008;68:503–12.
18. Nishiyama N, Kataoka K. Preparation and characterization of size-controlled polymeric micelle containing cis-dichlorodiammineplatinum(II) in the core. J Control Release. 2001;74:83–94.
19. Schroeder A, Honen R, Turjeman K, Gabizon A, Kost J, Barenholz Y. Ultrasound triggered release of cisplatin from liposomes in murine tumors. J Control Release. 2009;137:63–8.
20. Keskar V, Mohanty PS, Gemeinhart EJ, Gemeinhart RA. Cervical cancer treatment with a locally insertable controlled release delivery system. J Control Release. 2006;115:280–8.
21. Terwogt JMM, Schellens JHM, Huinink WWtB, Beijnen JH. Clinical pharmacology of anticancer agents in relation to formulations and administration routes. Cancer Treat Rev. 1999;25:83–101.
22. Li Y, Widodo J, Lim S and Ooi CP. Synthesis and cytocompatibility of manganese(II) and iron(III) substituted hydroxyapatite nanoparticles. J Mater Sci, 2011, doi:10.1007/s10853-011-5851-7.
23. Li H, Chang J. pH-compensation effect of bioactive inorganic fillers on the degradation of PLGA. Compos Sci Technol. 2005;65:2226–32.
24. Agrawal CM, Kyriacos AA. Technique to control pH in vicinity of biodegrading PLA-PGA implants. J Biomed Mater Res. 1997;38:105–14.
25. Martin C, Winet H, Bao JY. Acidity near eroding polylactide-polyglycolide *in vitro* and *in vivo* in rabbit tibial bone chambers. Biomaterials. 1996;17:2373–80.
26. Linhart W, Peters F, Lehmann W, Schwarz K, Schilling AF, Amling M, *et al.* Biologically and chemically optimized composites of carbonated apatite and polyglycolide as bone substitution materials. J Biomed Mater Res. 2001;54:162–71.
27. Chen X, Ooi CP. Hydrolytic degradation and drug release properties of ganciclovir-loaded biodegradable microspheres. Acta Biomater. 2008;4:1046–56.
28. Amado AM, Fiuza SM, Marques MPM, Batista de Carvalho LAE. Conformational and vibrational study of platinum(II) anticancer drugs: cis-diamminedichloroplatinum (II) as a case study. J Chem Phys. 2007;127:185104.
29. Chen X, Ooi CP, Lye WS, Lim TH. Sustained release of ganciclovir from poly(lactide-*co*-glycolide) microspheres. J Microencapsul. 2005;22:621–31.
30. Park TG. Degradation of poly(D, L-lactic acid) microspheres: effect of molecular weight. J Control Release. 1994;30:161–73.
31. Rouse JJ, Mohamed F, van der Walle CF. Physical ageing and thermal analysis of PLGA microspheres encapsulating protein or DNA. Int J Pharm. 2007;339:112–20.
32. Yoshioka T, Kawazoe N, Tateishi T, Chen G. *In vitro* evaluation of biodegradation of poly(lactic-*co*-glycolic acid) sponges. Biomaterials. 2008;29:3438–43.
33. Giunchedi P, Conti B, Scalia S, Conte U. *In vitro* degradation study of polyester microspheres by a new HPLC method for monomer release determination. J Control Release. 1998;56: 53–62.
34. Yung W-KA, Shapiro JR, Shapiro WR. Heterogeneous chemosensitivities of subpopulations of human glioma cells in culture. Cancer Res. 1982;42:992–8.
35. Lippard SJ. New chemistry of an old molecules: *cis*-$[Pt(NH_3)_2Cl_2]$. Science. 1982;218:1075–82.
36. Yotsuyanagi T, Usami M, Noda Y, Nagata M. Computational consideration of cisplatin hydrolysis and acid disociation in aqueous media: effect of total drug concentrations. Int J Pharm. 2002;246:95–104.
37. Sheindorf C, Rebhun M, Sheintuch M. A Freundlich-type multicomponent isotherm. J Colloid Interface Sci. 1981;79: 136–42.
38. Urano K, Koichi Y, Nakazawa Y. Equilibria for adsorption of organic compounds on activated carbons in aqueous solutions I. Modified Freundlich isotherm equation and adsorption potentials of organic compounds. J Colloid Interface Sci. 1981;81:477–85.
39. Chval Z, Sip M. Pentacoordinated transition states of cisplatin hydrolysis–ab initio study. J Mol Struct. 2000;532:59–68.
40. Rosca ID, Watari F, Uo M. Microparticle formation and its mechanism in single and double emulsion solvent evaporation. J Control Release. 2004;99:271–80.
41. Nagata F, Miyajima T, Yokogawa Y. Surfactant-free preparation of poly (lactic acid)/hydroxyapatite microspheres. Chem Lett. 2003;32:784–5.
42. Siepmann J, Elkharraz K, Siepmann F, Klose D. How autocatalysis accelerates drug release from PLGA-based microparticles: a quantitative treatment. Biomacromolecules. 2005;6: 2312–9.
43. Klose D, Siepmann F, Elkharraz K, Krenzlin S, Siepmann J. How porosity and size affect the drug release mechanisms from PLGA-based microparticles. Int J Pharm. 2006;314:198–206.
44. Miyajima M, Koshika A, Okada Ji, Ikeda M. Effect of polymer/basic drug interactions on the two-stage diffusion-controlled release from a poly(L-lactic acid) matrix. J Control Release. 1999;61:295–304.
45. Bontha S, Kabanov AV, Bronich TK. Polymer micelles with cross-linked ionic cores for delivery of anticancer drugs. J Control Release. 2006;114:163–74.
46. Ye H, Jin L, Hu R, Yi Z, Li J, Wu Y, *et al.* Poly (*γ*, *L*-glutamic acid)-cisplatin conjugate effectively inhibits human breast tumor xenografted in nude mice. Biomaterials. 2006;27:5958–65.
47. Bouissou C, Rouse JJ, Price R, Walle CFvd. The influence of surfactant on PLGA microsphere glass transition and water sorption: remodeling the surface morphology to attenuate the burst release. Pharm Res. 2006;23:1295–305.